Received: 5 March 2024 | Revised: 23 May 2024 | Accepted: 8 June 2024

DOI: 10.1002/app.55894

RESEARCH ARTICLE

Applied Polymer Science WILEY

Self-lubricating polyamide 6 and polyamide 6.6 microcapsule-based composites

Moritz Grünewald[1] | **David Herbig**[2] | **Michael Heilig**[2] | **Johannes Rudloff**[2] | **Martin Bastian**[2] | **Gunnar Engelmann**[3] | **Max Hirsekorn**[3] | **Alexandra Latnikova**[3]

[1]Fraunhofer Institute for Manufacturing Engineering and Automation, Stuttgart, Germany

[2]SKZ—German Plastics Center, Würzburg, Germany

[3]Fraunhofer Institute for Applied Polymer Research, Potsdam, Germany

Correspondence
Moritz Grünewald, thermoplastic processes, Fraunhofer Institute for Manufacturing Engineering and Automation IPA, Nobelstr. 12, 70569 Stuttgart, Germany.
Email: moritz.gruenewald@ipa.fraunhofer.de

Funding information
Bundesministerium für Wirtschaft und Klimaschutz, Grant/Award Number: 210707 BG

Abstract

Polymeric applications with extended service life and low energy loss due to friction are of great interest in conveyor and power transmission technology. Self-lubricating systems utilizing microcapsules hold significant potential for increasing energy efficiency and extending the operational life of these applications. This study focuses on synthesizing oil-filled microcapsules through in situ polymerization of polyamide and their incorporation in polyamide 6 and polyamide 6.6. Microcapsules with a core made of thermally stable lubricant Food Lube, and particle diameter D_{90} of 50 μm were synthesized and isolated as a free-flowing powder via spray-drying procedure. The resulting powder demonstrated high thermal stability (loss of 5% at 350°C) due to the high thermal stability of both core and shell materials. A compounding process utilizing a twin-screw extruder was developed to blend microcapsules into thermoplastic matrices. An injection molding machine forms tension rods. The composites' tribological properties are assessed through ball-on-disc tests conducted in both oscillation and rotation. The friction coefficient and wear rate of the composites experience a reduction of 79% and 56% for polyamide 6, as well as 77% and 75% for polyamide 6.6. Mechanical testing of the microcapsule composites reveals a decrease in mechanical properties.

KEYWORDS

friction, functionalization of polymers, polyamides, synthesis and processing techniques, thermoplastics, wear and lubrication

1 | INTRODUCTION

Polymer-based tribomaterials are widely used in the manufacturing of components such as sliders, switches, gears, or bearings in transmission systems. Plastic parts exhibit desirable characteristics such as good dry-running sliding and high-damping behavior. Their resistance to harsh chemical conditions and low density allows for widespread use in various applications.[1] To prolong the lifespan and minimize the maintenance of components

under tribological stress, plastics can be enhanced with different additives, fillers, and coatings.

One way to increase the wear resistance of plastic materials is by introducing an additional hard coating on the surface of the softer underlying substrate. Thus, in Raheem and Kareem,[2] NiCr coating was deposited onto the underlying epoxy composite substrate by flame-spray technique, leading to the significant reduction of friction coefficients, whereas the effects were even higher when an adhesion promoter (polyimide coating) was introduced. The friction coefficient of an epoxy composite was reduced from ca. 1 to ca. 0.4, and wear rate from 7 to 2×10^{-6} mg $\times$ $(cm)^{-1}$ at 100°C, which corresponds to 60% and 71%, respectively. However, this method requires elaborate equipment and an additional coating processing step. Another common method to increase the wear resistance of plastic parts is through the addition of solid additives to the polymer matrix. Nanosilica, molybdenum-disulfide (MoS_2), graphite, carbon fibers, and polytetrafluorethylene (PTFE) are known to reduce wear rates.[3–8] Solid additives are used where external application of lubricants is not possible, for example in transmission components in enclosed housings of power tools. In some applications, oily surfaces are not beneficial due to dust adhering the surface. PTFE is the most commonly used solid additive in tribologically stressed plastic components.[9] The friction reduction of PTFE is based on its low surface energy and ability to form stable transfer layers.[10] Due to the relatively low mechanical properties of PTFE, bulk-PTFE has a high wear-coefficient and is therefore often blended with mechanical tough materials. Metal-based solid additives can be used to improve tribological performance and often contain a molecular 2D layered structure that facilitates sliding over one another.[11] Nanosilica acts as a rolling third body in between the surfaces.[12] Depending on the tribological load spectrum (load, speed, type of movement, ...), the solid additives show varying degrees of friction reduction potential.[13] Compared with oils or greases, solid lubricants have less potential to reduce friction and wear.[14] Solid additives can be easily incorporated into plastics, while oils are more problematic to integrate. Microencapsulation of lubricants is a relatively new approach to incorporate oils into a polymer matrix as a pseudo-solid additive. Oil-filled microcapsules have the advantage that they can be processed like a solid additive. When mechanical wear is applied to the part surface, the capsule walls rupture, which releases oil, resulting in self-lubrication at the location where it is needed. The release of oil at the interface between the contacting bodies reduces the adhesive forces between them. Consequently, the friction and wear decrease, particularly when the parts in contact have a high ability to adhere to one another.

In recent years, self-lubricating materials containing microcapsules have received increasing attention. The function of oil-filled microcapsules is predominantly described in epoxy resin systems. Guo et al. encapsulated lubricant oil with poly(melamine-formaldehyde) and the resulting microcapsules were mixed with epoxy resins in varying amounts.[15] At a microcapsule concentration of 10 wt%, the coefficient of friction (COF) and wear decreased by 75% and 98%, respectively, compared with the unfilled material. It has been demonstrated that an increase in the number of microcapsules above a several threshold (approximately 10 wt%) does not result in a further reduction of tribological properties due to the softening and weakening effect of the microcapsules on the matrix.[16] It was also depicted that as the amount of microcapsules increased, the mechanical properties decreased, showing the possible limitation in the use of microcapsules in certain applications. The incorporation of oil-filled microcapsules into thermoplastic matrices has been described for several thermoplastics for example, in polyoxymethylene (POM), polypropylene (PP), and polybutylene terephthalate (PBT).[17–21] Armada et al. investigated a cospraying method of microcapsules and polyamide (PA).[22] Scanning electron microscopy (SEM) images of cross-sections revealed uniform distribution of non-destroyed capsules in the matrix. Tribological tests of reciprocating steel ball on the coating showed decreased COF from 0.47 to 0.14. Analysis of the wear track displayed wear debris inside the cracked capsules.[23] Li et al. investigated polydopamine-modified polysulfone/silica double-walled microcapsules in PA.[24] They found that incorporating 10 wt% microcapsules in a PA6 composite resulted in an 82% reduction in friction coefficient and an 88% reduction in specific wear loss compared with pure PA6. In a recent study, Li et al. synthesized and tested SiO_2 nanocapsules in PA6.[25] The compounds showed reduced tribological properties while mechanical properties remained constant. The processing of microcapsules beyond the laboratory scale has rarely been described. PA6.6 is a widely used polymer for tribological applications, but it has not been reported to be modified with lubricant-filled microcapsules.[26]

PA6 and PA6.6 are quite challenging materials for the filling with microcapsules due to the high melting and processing temperatures of 240–270°C. Our previous attempts to incorporate melamine-formaldehyde-shell microcapsules in PA6/PA6.6 have failed, and we observed the presence of the nonencapsulated oil on the surface of the pellets and/or injection-molded parts (not published results). Therefore, we decided to test highly thermally stable microcapsules with cross-linked aromatic PA shells in combination with a thermally stable oil-formulation Food Lube.

Compounding microcapsules with thermoplastic resin requires low shear processing conditions to prevent the release of the capsule core. It is necessary for the microcapsules to possess high thermal stability to endure the melting temperature during compounding. Due to the high processing temperatures of PA, high thermal stability of the capsules is mandatory. Therefore, a high vapor pressure of the oil and a high thermal degradation temperature of the capsule wall material are of great interest. To minimize thermal and shear stress, the residence time of the capsules should be kept short. A high chemical compatibility between the shell material and the matrix is beneficial for improved mechanical properties and dispersion ability. The injection molding process following can cause further stress on the capsules. If oil is released in the single-screw extruder, plasticizing may stop due to lack of frictional heat. A review of relevant literature reveals a lack of comprehension regarding the processes affecting thermoplastic/oil-filled microcapsule composites in scaled-up equipment.[17,27]

The objective of this paper is to provide an initial demonstration of the feasibility of synthesizing, incorporating, and testing lubricant-filled microcapsules with a PA-shell in thermoplastic PA. The microcapsules were blended in PA6 and PA6.6 matrix materials to obtain composites with self-lubricating properties. These technical thermoplastic resins display semi-crystalline properties, which are used in a wide range of tribological applications. The microcapsules were mixed in a continuous process and formed using a corotating twin-screw extruder and injection molding system. Fabricated tension rods underwent tribological testing involving steel-ball on plate tests conducted under both oscillation and rotation modes. Mechanical properties of the composites were analyzed using tensile tests. The findings of this study provide a firm basis for further lubricant-filled microcapsule composite studies.

2 | MATERIALS AND METHODS

2.1 | Materials

To enable potential use in the field of food technology, we selected and encapsulated "Food Lube R-5555" a low-viscosity oil certified for food and pharmaceutical applications (manufactured by Riedel Schmierstoffe, Germany). 1,3,5-Benzenetricarbonyl chloride (BTCC), isophorone diamine (IPDA), Mowiol 8–88 Polyvinyl alcohol (PVA), NaOH, ethanol, and ethyl acetate (EA) were purchased from Sigma-Aldrich and used as received.

PA6 (Alphalon 27C, groupa azoty, Poland) and PA6.6 (Radipol A40, Radici Group, Poland) were used as thermoplastic matrices for the compounds. Both polymers are noncolored and easy-flowing grades. As unmodified references PA6 (Ultramid B3L, BASF, Germany) and PA6.6 (Radipol A40, Radici Group, Poland) were used. Prior to using, the materials, they were dried according to supplier advise.

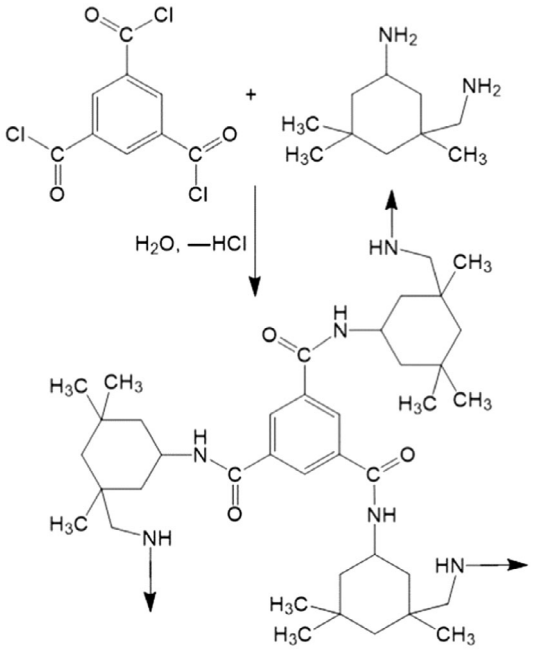

FIGURE 1 Reaction between 1,3,5-benzenetricarboxylic acid chloride and isophorone diamine leading to the formation of polyamide shell.

2.2 | Synthesis of microcapsules

The PA-microcapsule (PA/MC) synthesis procedure was inspired by the proceeding described in Poncelet et al.[28] The microcapsules were produced via interfacial polymerization between BTCC and IPDA (Figure 1).

The microencapsulation process starts with the preparation of three solutions, the oil phase (containing acid chloride, EA, and the lubricant), continuous water phase (containing emulsion stabilizer), and second aqueous phase (10% NaOH, containing the amine). The oil phase is added to the continuous aqueous phase and two phases are homogenized by using rotor-stator type of a homogenizator (Ultra-Turrax). After that, the second aqueous phase is added and the mixture is further stirred with a paddle mixer for 2 h. The process is schematically shown in Figure 2.

To prepare the continuous phase, 8 L of a 1% solution of PVA was prepared by dissolving the corresponding amount of the polymer in water at a temperature of 70°C. To prepare the oil phase, 900 g of lubricant Food

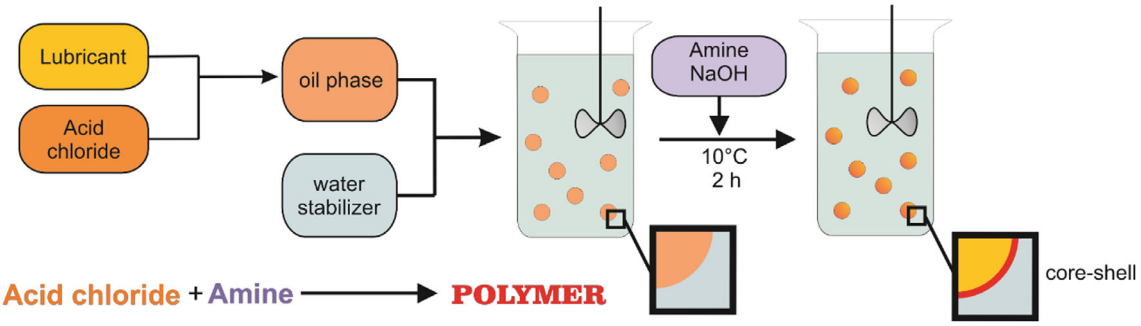

FIGURE 2 Schematic representation of the microencapsulation process in polyamide. [Color figure can be viewed at wileyonlinelibrary.com]

Lube were filled into a 2 L ground-glass Erlenmeyer flask to which 150 mL EA and 135 g BTCC were added and the mixture was stirred on a magnetic stirrer until all the BTCC was dissolved (several minutes). Three hundred twenty grams IPDA was added in portions to 320 g ice-cool 10 wt% NaOH while stirring and cooling so that the temperature stays below 20°C. The resulting emulsion was kept stable with the aid of a magnetic stirrer.

A stainless-steel reactor was filled with 8 L of 1% PVA solution. Then the paddle stirrer was switched on and the ice water cooling was activated. After the temperature of 6°C was reached, the Ultra-Turrax was started (10,000 rpm) and the oil with acid chloride was added slowly over 5 min. The temperature in the reactor was kept below 10°C by external cooling. Then approximately 0.2 g phenolphthalein was added to the emulsion to track the changes of the pH in the aqueous phase.

The IPDA/NaOH emulsion was then carefully added stepwise over 20 min. After adding the entire amount of amine and alkali, the batch was stirred with the paddle stirrer for 2 h. After that the mixture was left standing for 10 h and neutralized with 0.5 molar sulfuric acid. The resulting suspension was vacuum filtered on a paper filter and washed three times with 2 L of water. The filter cake was then dispersed in 8 L of water and spray-dried. The air temperature at the inlet was 240°C while the outlet temperature was 75 ± 5°C. The total amount of isolated particles was approximately 1 kg. Due to the flexibility of the shell the microcapsules could not be isolated by simple air-drying (which is possible for the polyurethane and melamine-formaldehyde microcapsules with the similar size).

After washing and filtration, 5 g of the microcapsule cake was extracted in 50 g EA under intensive magnetic stiring overnight for three times. It was filtered, spread on a glass dish and dried by letting it stand under a hood overnight and was further used for thermogravimetric and FT-IR analysis.

2.3 | Sample preparation

Material compounding and injection molding were performed on kg-scale. Figure 3 shows a schematic illustration of the sample preparation process. Capsule concentrations were chosen based on laboratory-scale experiments. The preliminary study examined the effects of capsule concentrations between 1 and 15 wt% on the stability and reproducibility of process conditions. At higher capsule concentrations, in particular the injection molding process is highly unstable due to the released oil, while remelting in the single-screw extruder. The capsule concentrations used in the study represent the maximum possible capsule concentrations with constant process conditions. The maximum oil concentrations employed were 8 and 5 wt% in PA6 and PA6.6, respectively. With a capsule core content of 80 wt%, this corresponds to a capsule concentration of 10 and 6.25 wt% in PA6 and PA6.6.

2.3.1 | Compounding

A co-rotating twin-screw extruder (ZSK 26 Coperion, Germany) was utilized for compounding. The main feeder was employed for the gravimetric dosing of the matrix polymer while the microcapsule powder was introduced through a side feeding system located at the tenth barrel out of 11 in the extruder. The extruder used had a screw diameter of 26 mm, a length/diameter (L/D) ratio of 44 and its screw design was developed specifically for the sample preparation. A kneading block with paddles at a 45-degree angle was placed immediately after capsule feeding to mix the capsule/polymer melt. The shear load applied to the microcapsules had to be minimized to avoid premature release of the lubricating oil and ensure even distribution within the matrix. Compounding tests were conducted with throughputs of 15 kg/h and rotational screw-speed of 200 min^{-1}.

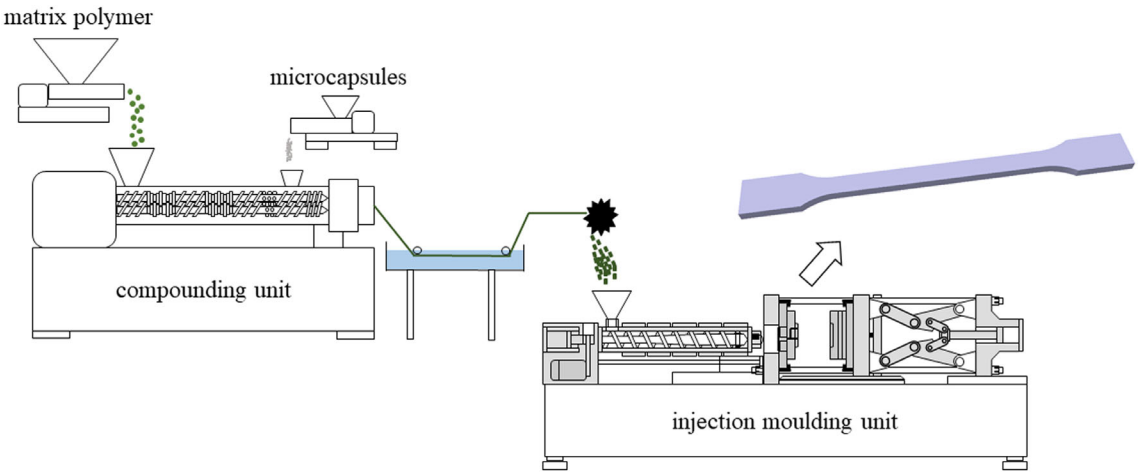

FIGURE 3 Schematic illustration of the sample preparation by compounding microcapsules via side-feeding system and injection molding of tensile specimens type DIN EN ISO 527 1A. [Color figure can be viewed at wileyonlinelibrary.com]

TABLE 1 Barrel-temperatures of the compounding-extruder from main-feeder (1) to nozzle (11) in celsius degree.

Barrel	1	2	3	4	5	6	7	8	9	10[a]	11
PA6 + PA/MC 8/°C	200	235	225	225	225	225	220	220	220	220	230
PA6.6 + PA/MC 5/°C	260	275	275	275	275	275	270	270	265	265	265

[a]Capsule side-feeding system.

TABLE 2 Temperatures of the injection molding unit from feeder (1) to nozzle (6) in Celsius degree.

Barrel	1	2	3	4	5	6	Tool
PA6 + PA/MC 8/°C	70	230	235	240	245	245	60
PA6.6 + PA/MC 5/°C	70	255	260	265	270	270	80

Resulting polymer strands were cooled in a water bath and granulated while cold as a strand. Extruder-barrel temperatures are set according to Table 1. Each barrel is equipped with a temperature sensor that regulates the heat power output.

2.3.2 | Injection molding

The pellets were molded using injection (KM 160-750PX, Krauss Maffei, Germany) into tension rods of type 1A (DIN EN ISO 527). The machine used was equipped with a single-screw with three zones and a diameter of 35 mm. PA6 and PA6.6 were molded using injection pressure of 440 and 278 bar, respectively. The temperatures were set and sensor-controlled according to Table 2. To ensure processability, 100 samples were produced for each material.

2.4 | Characterization

2.4.1 | Laser diffraction particle size analysis

All light scattering measurements of microcapsules were performed using a LS 13 320 SW (Beckmann Coulter, USA) to analyze particle size of the capsules. Low angle forward light scattering with optional PIDS (polarization intensity differential scattering) technology was used.

2.4.2 | Optical microscopy

Optical microscopy pictures were recorded on a Zeiss Axioskop A1 by using a Zeiss AxioCam 506 color detector (Carl Zeiss, Germany). The light was given by compact light source HXP 120 V.

2.4.3 | Thermogravimetric analysis

Thermo gravimetric analysis (TGA) was carried out on a TGA 2 LF/1100/885 from Mettler (USA) with the heating rate of 10 K min^{-1} under nitrogen atmosphere. The weight of each sample did not exceed 10 mg.

2.4.4 | FT-IR spectroscopy

FT-IR spectroscopy (FT-IR) measurements were carried out with a Thermo Nicolet NEXUS 470 FT-IR spectrometer (Thermo Fisher Scientific, USA) with DTGS/KBr detector equipped with total attenuated reflectance accessory with germanium crystal. Automatic atmosphere correction has been performed for each measurement. Spectra were recorded at room temperature between 500 and 3500 cm^{-1} with 2 cm^{-1} resolution.

2.4.5 | Scanning electron microscopy

The microcapsule powder and the processed polymer-microcapsule compounds were analyzed via SEM (Supra 40 VP, Carl Zeiss, Germany). SEM images of the compounds were made on fractured surfaces of the tensile test specimens.

2.4.6 | Mechanical properties

The influence of the microcapsules on the mechanical properties were characterized based on tensile tests (Z010, Zwick/Roell, Ulm, Germany) according to DIN EN ISO 527 (number of tests $n = 5$). The strain was measured using a multiXtens-system. The specimens were tested with a speed of 50 mm × min^{-1} (Young's modulus at 1 mm × min^{-1}) and a preforce of 5 N. Young's modulus, ultimate tensile strength, and elongation at break were tested and analyzed.

2.4.7 | Tribological properties

The tribological tests were conducted using a ball-on-disc configuration under standard conditions (23°C, 50% relative humidity). The clamping area of the tension rods were used as one body of the tribological setup. The counter body was a 100Cr6 steel ball with a radius r of 3 mm and a roughness of Ra 0.032 µm. Both contact-partners were cleaned using isopropyl-alcohol before analysis. Tests were performed in rotation and in oscillation mode to investigate tribological performance under different system parameters. Rotational tests were performed under linear speed of 50 cm × s^{-1} and a normal load of 10 N. Each compound ($n = 4$) was tested over a distance of 5 km and a track radius of 8 mm. Tests in oscillation mode were performed under a normal load of 30 N, amplitude of 10 mm, speed of 1 Hz, and a test-duration of 10,000 cycles. The average COF was determined by using the last 20% of the tested distance, therefore the effects of friction during running-in can be neglected. A single representative COF profile is presented for each sample.

The wear loss of the analyzed tribological system is solely described by the wear of the polymeric body since the steel ball did not show any wear phenomena. The wear volume was characterized by using a 3D profiling microscope (S neox, Sensofar, Terrassa, Spain) and MountainsMap 10 (Digital Surf, Besançon, France) according to Ayerdi et al.[29] The wear track depth of the rotation-tested samples was mainly for the PA6.6 samples too low to be characterized by the method described in Ayerdi et al.[29] Therefore, the wear was characterized by measuring the wear track width s at eight distinct positions and calculating the wear volume according to ASTM G99-17 by means of Equation (1) using radius of the steel ball $r = 3$ and track radius R of 8 mm.

$$V_{\text{wear}} = \frac{\pi \times s^3 \times R}{6r}. \quad (1)$$

The wear volume of the oscillation-tested samples was characterized by 3D-profiling. First the 3D-profile of the wear track and its surroundings was measured using confocal microscopy with a 10× objective lens. Next, the tilting of the wear track surrounding surface was leveled using a mathematical operator (gaussian function 3rd degree). Lastly, the wear volume V_{wear} was calculated by subtracting the wear track topography from the leveled surrounding surface using MountainsMap 10.

The calculation of the wear rate w_s has been done according to Equation (2) by setting the wear volume V_{wear} into proportion of the normal force F_N and tested distance S.

$$w_s = \frac{V_{\text{wear}}}{F_N \times S}. \quad (2)$$

3 | RESULTS AND DISCUSSION

3.1 | Microcapsules properties

The optical microscope images and the particle size distribution of the microcapsules directly from the synthesis

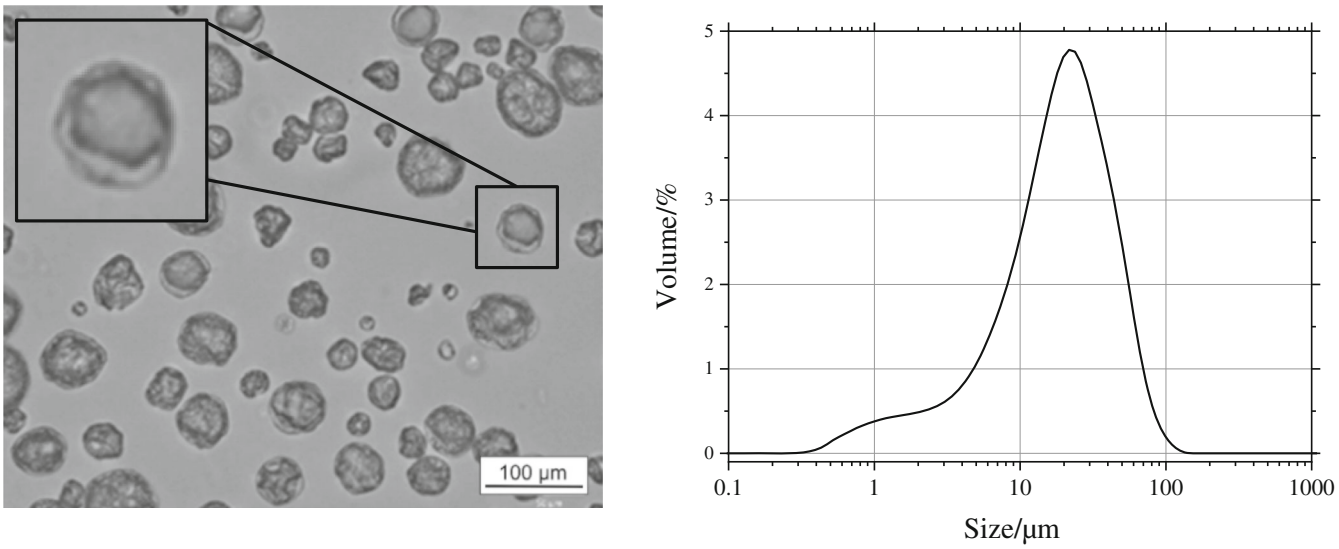

FIGURE 4 Optical microscope images (left) and particle size distribution (right) of PA-based microcapsules containing lubricant Food Lube. The insert presents one magnified microcapsule for better visibility of the capsule membrane.

are shown in Figure 4. The size distribution Figure 4 of microcapsules was bimodal with the main peak at 19 µm and a shoulder around 1 µm. The D_{90} value was equal to 47 µm. These values are in agreement with the optical microscope observations confirming relatively broad particle size distribution. Bimodal particle size distributions are beneficial for enhanced particle distribution and packing density in the matrix. Sun et al. investigated the tribological effects of self-healing coatings containing nanocapsules with different sizes.[30] Their findings indicated that smaller particle sizes produced rougher plowing and microcracks. Khun et al. demonstrated that the incorporation of larger microcapsules resulted in a more pronounced reduction in friction, due to a higher amount of released oil.[31] By varying the size and morphology of the microcapsules, the stability of the capsules can be manipulated. It is essential that the microcapsules are stable enough to withstand the compounding and manufacturing processes without being damaged. Conversely, the oil must be released instantaneously during the subsequent application.

The transparent shells (part of shells) of the microcapsules can be observed, which is not typical for the microcapsules prepared by interfacial polymerization[21] and resemble more the typical images obtained for complex coacervates.[32] Like coacervates, the prepared microcapsules also seem to be flexible and elastic when pressed with the spatula between the cover glass and the microscope slide, tend to rather deform than rupture under pressure and rupture if the pressure is high enough. This allows us to assume that the formed PA shell is swollen with considerable (we assume more than 100 wt%) amounts of water. This makes the shells thicker and more flexible. Due to this flexibility, microcapsules agglomerate when dried in air. Due to this reason, they were spray-dried in order to achieve the dry free-flowing powder.

The mechanical behavior and appearance of the microcapsules differs from that of PA microcapsules prepared by other authors. Thus, in[33] fully aliphatic microcapsules with toluene core were prepared by interfacial polymerization. The air-dried microcapsules observed via SEM are not spherical; their shape suggests that microcapsule wall is very thin and remained flexible until most of the core material has been evaporated. A comparable picture can be observed in Chen et al.,[34] where the microcapsules dried by conventional drying in air and by freeze-drying were compared in SEM. Freeze-drying, in contrast to air-drying, led to nearly spherical particles. The thickness of the shell is in both cases extremely low and cannot be observed with optical microscope. The morphology of microcapsules under the optical microscope rather resembles the one presented in[35] where the initially formed PA shell was let to reswell in water, after which the polymerization could continue and highly swollen in water stable shells clearly visible in the microscope could be observed. The thermal stability of microcapsules is similar to the one demonstrated in Mytara et al.,[33] where double polymerization process has been used.

Figure 5 shows the SEM image of the spray-dried microcapsules. In contrast to microscope images, the microcapsules are nonspherical, and it is in fact not easy to recognize the original core-shell structure in the resulting agglomerates. It can be assumed that the flexible microcapsule shells are considerably distorted and

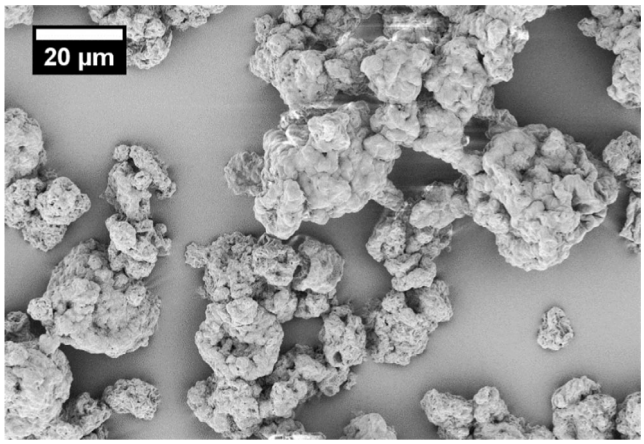

FIGURE 5 SEM-image of PA microcapsules with a magnification of 4000.

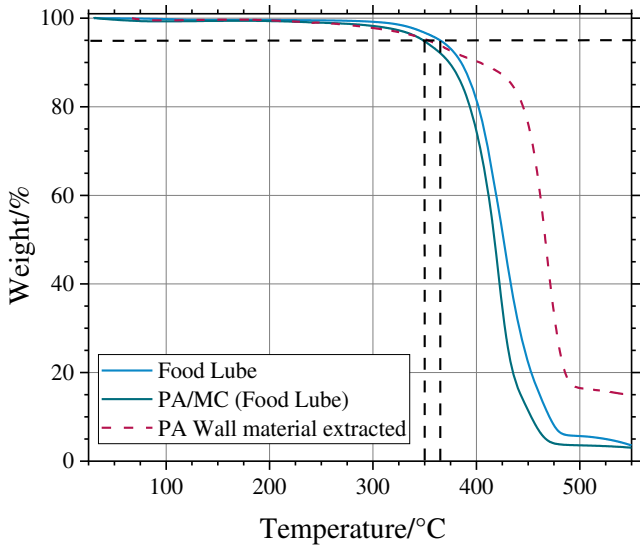

FIGURE 6 Thermogravimetric analysis of lubricant Food Lube, polyamide (PA)-based microcapsules, and capsule wall material left after the extraction of the core material. [Color figure can be viewed at wileyonlinelibrary.com]

stretched during the fast spray-drying process and solidify in form of folds and irregular formations. However, the quality of the powder was very good, and no oily feel could be observed meaning that most of the oil droplets were covered with a hard polymer shell. Redispersion of the powder in water leads to the suspensions, in which no free oil droplets could be observed by optical microscopy (appear as perfectly spherical objects in contrast to microcapsules, which have a more complex shape).

TGA shows that Food Lube is very thermally stable with 5 wt% weight loss at 365°C (Figure 6). In fact, the lubricant oil is more thermally stable than the PA wall material (350°C) and microcapsules (350°C), with regard to the same weight loss. It is notable that PA has two

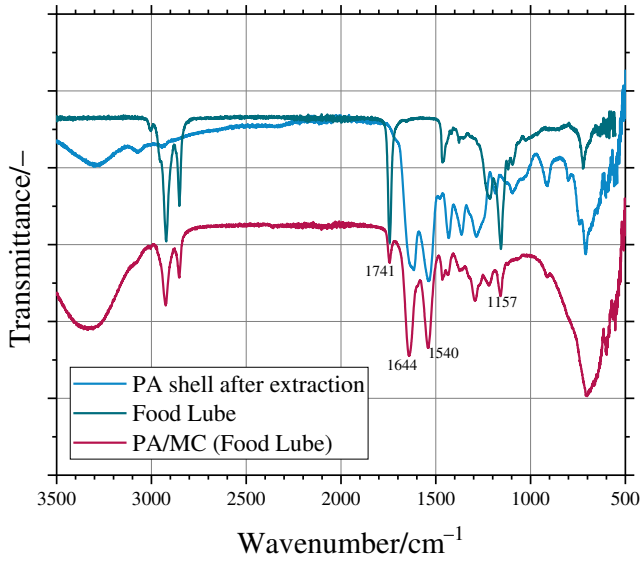

FIGURE 7 FT-IR spectra of Food Lube, polyamide (PA)-based microcapsules, and capsule wall material left after the extraction of Food Lube. [Color figure can be viewed at wileyonlinelibrary.com]

weight loss steps, a comparatively small one between 300 and 400°C (ca 10 wt%) and the main step between 450 and 500°C (ca. 70 wt%). The first step might be due to not completely extracted lubricant or due to incomplete polymerization of the PA.

The microcapsules are slightly less thermally stable than the lubricant and unexpected have less ash. This we have observed also for some other systems and one possible explanation of the phenomenon is that microcapsules have considerably higher surface area than the drop of the lubricant in a pan used for TGA analysis. The porous structure of microcapsules preserves until the decomposition of PA above 450°C, while in case of the lubricant a much denser film with small outer surface could be formed during the temperature rise. The chemical transformations happening at high temperatures can be affected by these structural differences and thus the differences in evaporation speed and ash content can arise.

The FT-IR analysis of the same samples shows that some rests of lubricant might be still present in the extracted specimens (Figure 7).

The peak at 1741 cm^{-1} can be assigned to the C═O stretch, the peak at 1157 cm^{-1} to C—O stretch in an aliphatic ester,[36] which are clearly present in the spectra of Food Lube and microcapsules and are much less pronounced (but recognizable) in the spectra of the extracted PA wall material.

The peak at 1644 cm^{-1} can be assigned to amide C═O, and the peak at 1540 cm^{-1} to the in-plane N—H bend typical for aromatic PA.[36] They are clearly present in the spectra of microcapsules and extracted shells, but not in the spectrum of Food Lube.

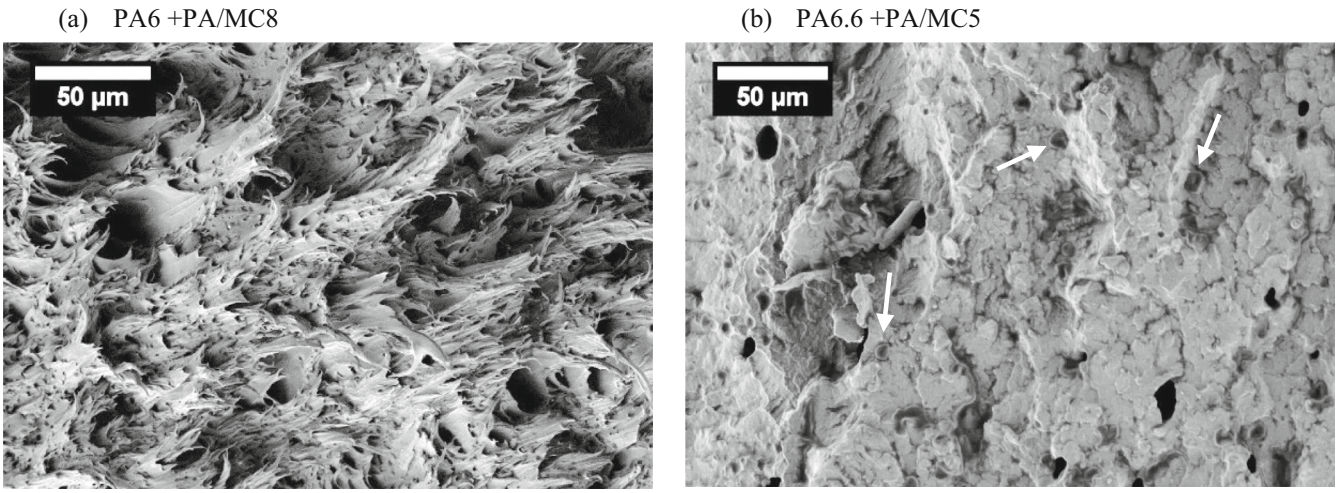

FIGURE 8 SEM images with a magnification of 1000 of thermoplastic composites (a) PA6 and (b) PA6.6 (arrows indicate undamaged capsules). The images show the surfaces of fractured tensile bars.

3.2 | Composites properties

While preparing the sample, the leakage of oil could not be detected at the compounding unit or the injection molding unit. A substantial oil release during the process results in significant injection molding problems, due to frictional conveying issues. Process parameters could be kept unchanged during processing of 100 specimens.

Figure 8 displays SEM images of fractured thermoplastic composite tensile bars. The surfaces exhibit different characteristics due to the contrasting fracture mechanisms of PA6.6 and PA6. It was not possible to identify microcapsules in the PA6 sample, even at higher magnifications. However, undamaged capsules were detected in the PA6.6 sample. Released oil was not detected in both samples. No agglomerates of microcapsules were obseved in the matrix during the preparation of the SEM image. A higher concentration of microcapsules at the surface of the samples is advantageous for tribological properties. The analysis of the samples by nondestructive micro-computer tomography (µCT) did not yield more detailed microcapsule distribution data due to the similarity in material density values.

3.2.1 | Mechanical properties

In Figure 9 the mechanical tensile properties of unfilled and microcapsules-filled PA6 and PA6.6 are shown. The addition of microcapsules in PA6 leads to reduced mechanical properties. The Young's modulus decreases by 21% to 2030 ± 35 MPa and ultimate tensile strength by 24% to 47 ± 0.20 MPa. Elongation at break values remains constant within the standard deviation 39% ± 9%. The reduction in the mechanical properties of microcapsule composites is therefore of a similar magnitude to other microcapsule-filled composites.[21] In comparison with PA6, PA6.6 displays a more rigid material characteristic with higher Young's modulus and lower elongation at break values. The presence of microcapsules results in reduced tensile properties. Young's modulus, ultimate tensile strength, and elongation at break exhibit values of 2900 ± 30 MPa (−8%), 64 ± 1 MPa (−18%), and 4.5% ± 1.1% (−82%), respectively. The reduction extent of the decrease in elongation at break is discernible. The cause for this cannot presently be determined for this material system.

The mechanical properties of PA6 + PA/MC8 are lower compared with an industrial PA6 grade with a PTFE amount of 10 wt%.[37] The Young's modulus and tensile strength of the commercial grade are 2200 and 58 MPa, respectively, and therefore up to 20% higher compared with the microcapsule-filled composite. Rudresh and Ravikumar investigated the mechanical properties of PA6.6 filled with 20 wt% PTFE. The results indicate a tensile strength of 66.5 MPa, which is within the same range as the microcapsule-filled PA6.6 composite studied in this investigation.[38] The Young's modulus exhibited a lower value (1040 MPa) compared with the PA6.6 + PA/MC5 sample. The high tribological effectiveness of microcapsules enables the mechanical properties to be maintained within the same range as other tribologically modified PA.

The reduced mechanical properties of microcapsule-filled composites may restrict their use in applications where higher structural loads are present. To address this limitation, Khun et al. incorporated additional carbon fibers into an epoxy matrix, thereby achieving both high

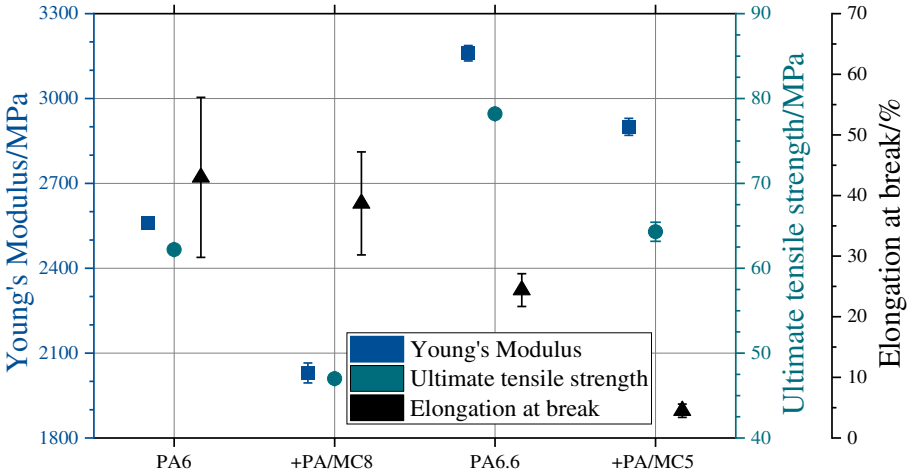

FIGURE 9 Mechanical properties of PA6 and microcapsule-filled PA6. [Color figure can be viewed at wileyonlinelibrary.com]

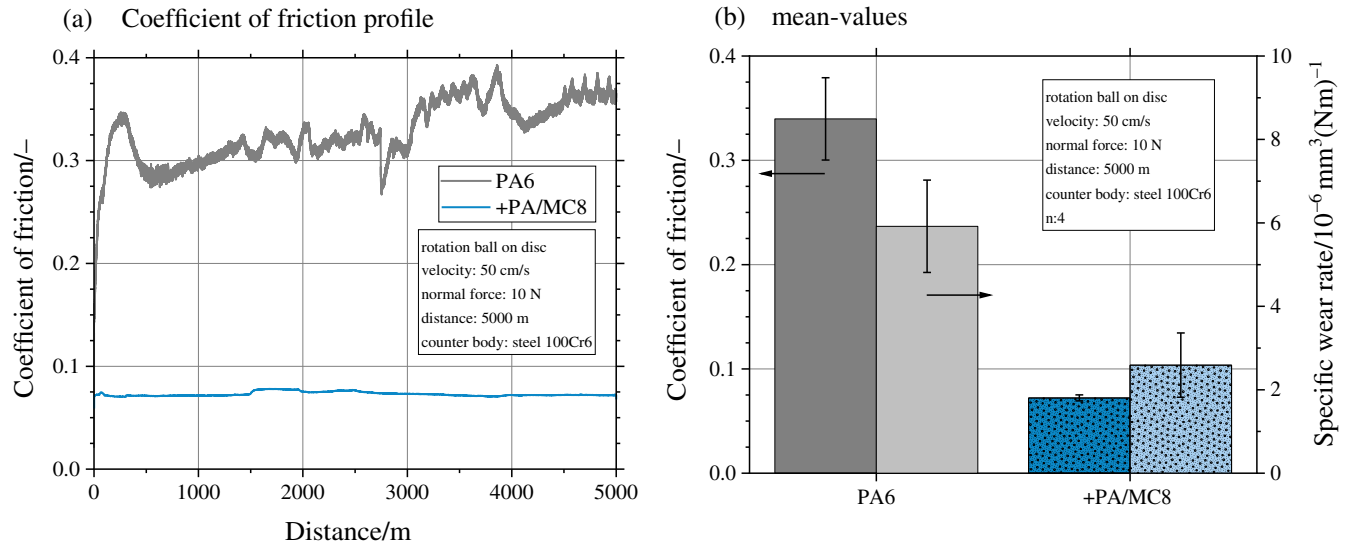

FIGURE 10 (a) Coefficient of friction (COF) profile and (b) mean COF and wear rates of PA6 and microcapsules-filled PA6 (+PA/MC8) samples tested against steel 100Cr6 ball. [Color figure can be viewed at wileyonlinelibrary.com]

tribological and mechanical properties.[39] This approach is of significant interest for testing in PA matrices containing microcapsules as well. If fiber reinforcement is not applicable in the later application, reduced amount of microcapsules can be used to limit the mechanical weakening effect of the microcapsules.

3.2.2 | Tribological properties

The rotational frictional analysis results are presented in Figure 10. The sample profiles of each composite represent the typical characteristics of that composite. No significant differences are observed between the samples. The COF profiles exhibit different characteristics from the beginning. The sample filled with microcapsules had an almost constant COF; however, the unfilled PA6 sample showed greater variation over the tested distance. The higher variations in the COF were due to the unstable formation of a transfer layer, as reported in Panin et al.[40] The profile of the microcapsule-filled sample demonstrates the high effectivity of the lubricant. The determined values of the mean COF and wear rate are shown in Figure 10b. The addition of microcapsules leads to a reduction of the averaged COF-values by 79% from 0.34 $\pm$ 0.04 to 0.07 $\pm$ 0.01 compared with the unfilled PA6 sample. Along with the reduction of COF, the lubricant-filled microcapsules resulted in a reduction of the wear rates as shown in Figure 10b. The specific wear rates of PA6 and PA6 + PA/MC8 are 5.9 $\pm$ 1.1 and 2.6 $\pm$ 0.7 $\times$ 10^{-6} $mm^3 \times (Nm)^{-1}$. Du-Xin et al. investigated the tribological effects of solid lubricants in PA6 in rotation against a steel counter surface. Their findings indicated that PTFE-based composites were most effective in

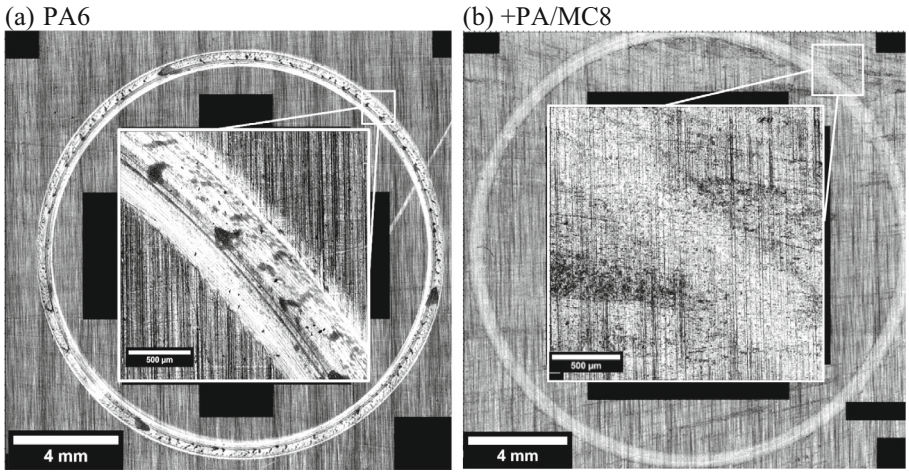

FIGURE 11 Microscopic images of (a) PA6 and (b) microcapsules-filled PA6 (+PA/MC8) after rotational tribological measurement tested against steel 100Cr6 ball.

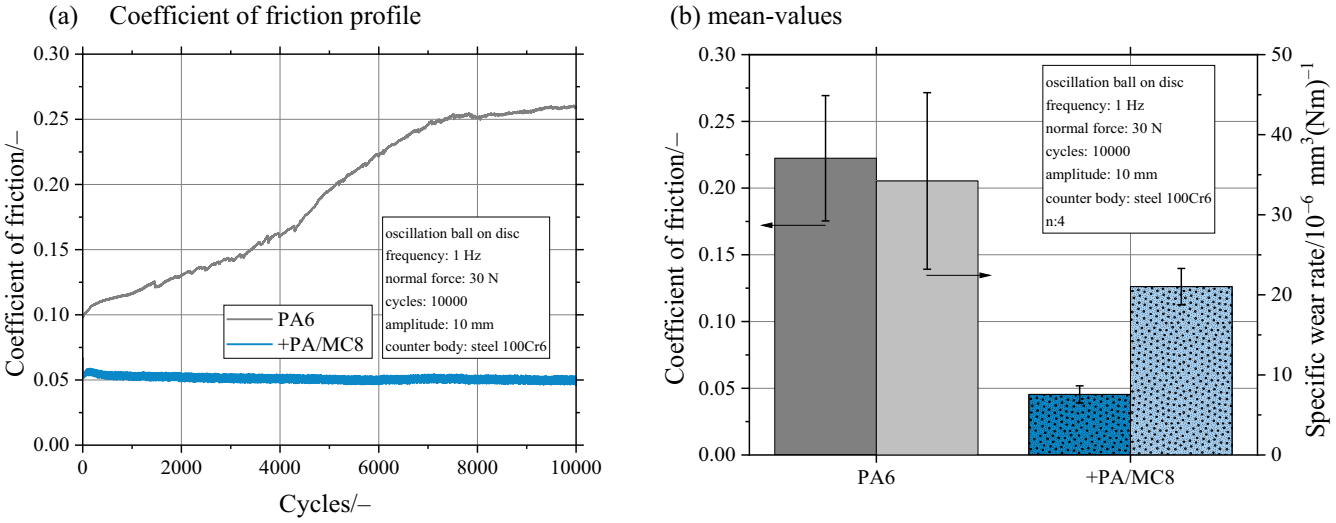

FIGURE 12 (a) Coefficient of friction (COF) profile and (b) mean COF and wear rates of PA6 and microcapsules-filled PA6 (+PA/MC8) samples tested against steel 100Cr6 ball. [Color figure can be viewed at wileyonlinelibrary.com]

reducing COF and wear rate at lower loads. Specifically, incorporation of 8 wt% PTFE led to a reduction in friction from 0.11 to 0.05. Furthermore, the incorporation of 2 wt % PTFE resulted in a wear rate reduction of 78%.[41]

Figure 11 shows microscopic images of the PA6 samples wear tracks. The wear track of the unfilled PA6 sample exhibits multiple grooves caused by fatigue and adhesive wear of the polymer, mainly located in the center of the wear track. In contrast, the capsule-filled sample displays a much smoother surface in the contact area, which can be attributed to the lubrication that mainly prevents adhesive wear of the polymer.

In Figure 12 the tribological testing of the PA6 in oscillating mode is shown. The friction profile of both samples over 10,000 cycles is presented and representative for each composite. The reference sample exhibits an increasing COF up to 8000 cycles, while the microcapsule-filled sample maintains a nearly constant COF throughout the entire test. The addition of the lubricant-filled microcapsules reduced the COF by 80% from 0.22 ± 0.05 to 0.05 ± 0.01. The wear rate of the polymeric partner reduced by 38% from 34.2 ± 11.0 to 21.0 ± 2.3 × 10^{-6} mm^3 × $(Nm)^{-1}$. Sathees Kumar and Kanagaraj conducted an investigation into the effectiveness of graphite as a solid additive in reducing friction and wear in rotational steel contact.[42] Their findings indicated that the addition of 20 wt% of graphite was the most effective and lead to a friction reduction at 30 N from 0.3 to 0.14 and wear rate reduction from 6.8 to 4.1 10^{-3} mm^3 × $(Nm)^{-1}$. The results of the frictional tests indicate that graphite is less effective than lubricant-filled microcapsules in reducing the COF.

In Figure 13 3D images of the wear tracks are displayed. The height of the investigated sample area is color-coded. The darker the blue color, the deeper the wear track. The capsule-filled sample shows a less deep

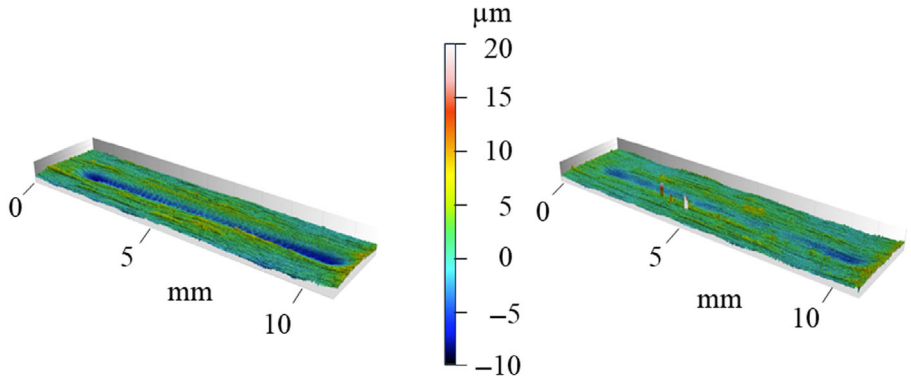

FIGURE 13 Microscopic 3D-images of (a) PA6 and (b) microcapsules-filled PA6 (+PA/MC8) after tribological oscillation measurement tested against steel 100Cr6 ball. [Color figure can be viewed at wileyonlinelibrary.com]

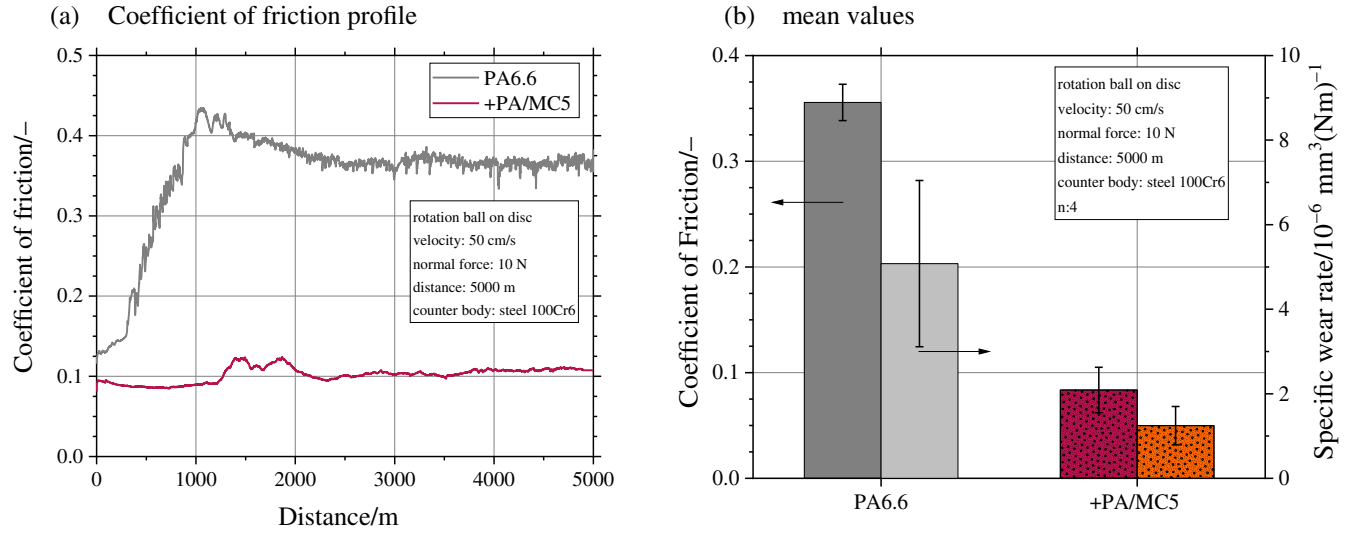

FIGURE 14 (a) Coefficient of friction (COF) profile and (b) mean COF and wear rates of PA6.6 and microcapsules-filled PA6.6 (+PA/MC5) samples tested against steel 100Cr6 ball. [Color figure can be viewed at wileyonlinelibrary.com]

wear track. The depth of the wear track of the PA6 sample is about 10 µm. The highest wear occurs for both samples at the reversal points at the ends of the track. Here counter body accelerates the most. Differences in wear depth are more pronounced for the capsule-additivated sample.

The tribological properties of PA6.6 samples are displayed in Figure 14. The COF profiles are representative for each composite and show a divergent behavior. The COF of the unfilled PA6.6 sample exhibits a sharp increase during the first 1000 meters of testing followed by a gradual decrease until reaching a plateau. The sample filled with microcapsule has a nearly constant COF over the tested distance and no running-in behavior was detected. The averaged values of unfilled and filled sample show decreased COF by 77% from 0.36 ± 0.02 to 0.08 ± 0.02. Thus, the COF reduction is in the same order as PA6 with a smaller number of microcapsules. The wear rate is reduced by 75% from 5.1 ± 2.0 to $1.2 \pm 0.5 \times 10^{-6}$ mm^3 × (Nm)$^{-1}$. Wang et al. conducted a study investigating the tribological properties of UHMWPE (ultra-high-molecular-weight polyethylene) filled PA6.6. UHMWPE was blended by a cotwin-screw extruder with a content up to 40 wt%. Lowest COF and wear rates were observed with an UHMWPE content of 10 wt% by forming a transfer layer on the steel counterpart. The COF and wear rate were reduced by up to 65% and 74%, respectively.[43]

Figure 15 shows microscopic images of the wear tracks of PA6.6 samples. The wear track of the unfilled PA6.6 sample contains grooves in the contact area. This is probably due to abrasive wear. The wear of the microcapsule-filled PA6.6 is only visible by the difference in gloss and not by the profilometer. The original roughness of the sample caused by the injection molding tool is detectable in the wear track as well. Microcapsules are distributed finely on the surface of the sample, resulting in an initial reduction of friction and wear of the polymeric body.

Figure 16 displays the tribological results in oscillation mode. The COF-profiles are representative for each

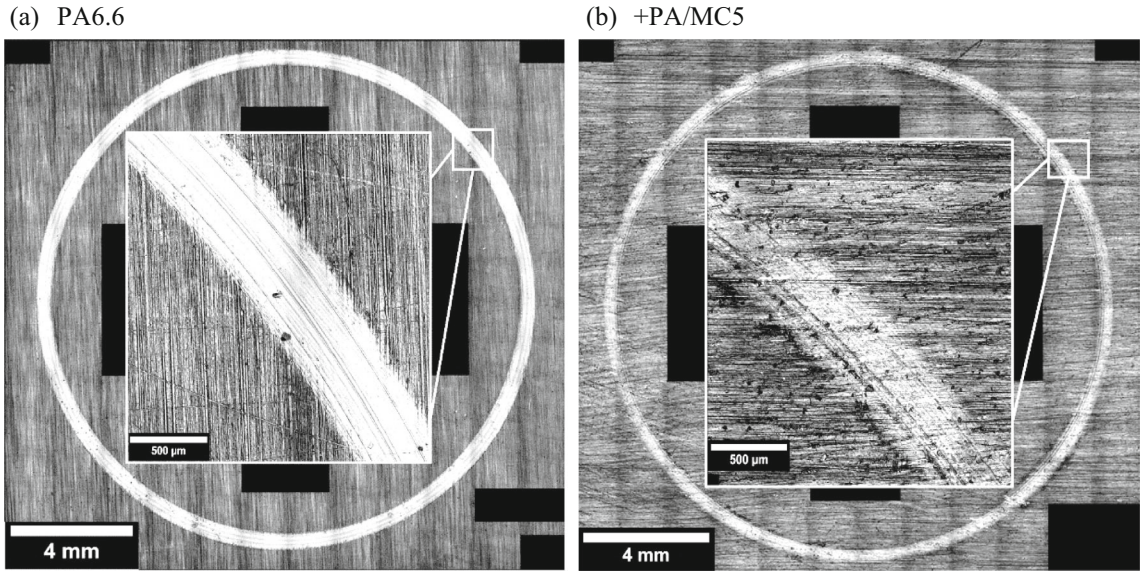

FIGURE 15 Microscopic images of PA6.6 and microcapsules-filled PA6.6 (+PA/MC5) after rotational tribological measurement tested against steel 100Cr6 ball.

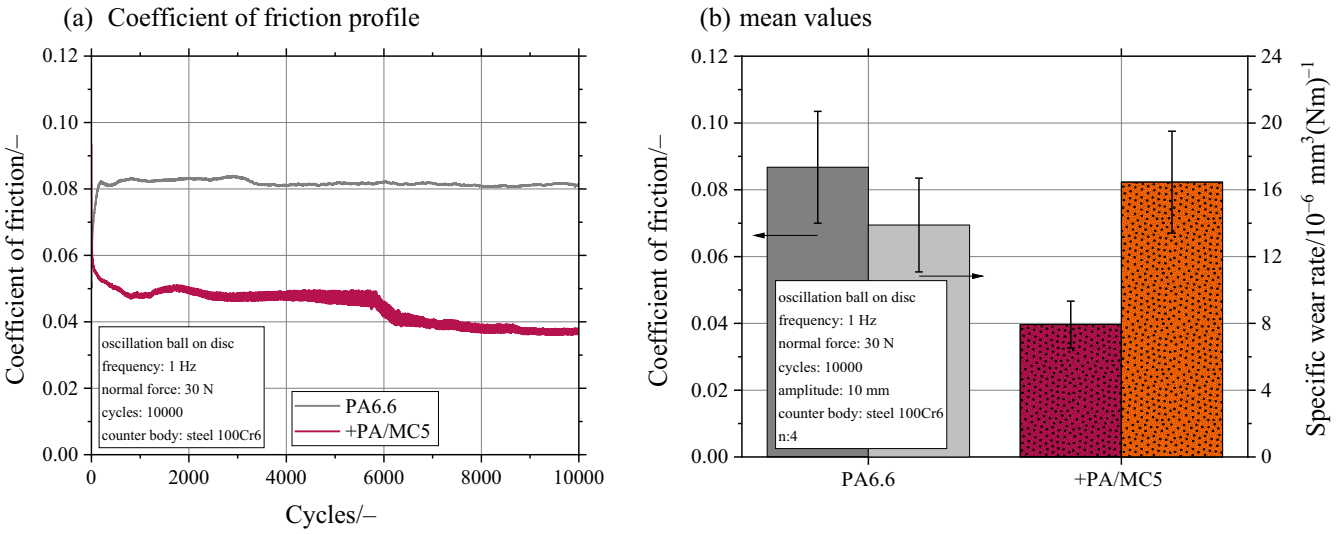

FIGURE 16 (a) Coefficient of friction (COF) profile and (b) mean COF and wear rates of PA6.6 and microcapsules-filled PA6.6 (+PA/MC5) samples tested against steel 100Cr6 ball. [Color figure can be viewed at wileyonlinelibrary.com]

composite and show for both samples nearly steady values. While the PA6.6 sample shows almost no deviations, the COF of the microcapsule-filled sample drops slightly with an increasing number of cycles. The mean COF is reduced by the addition of microcapsules by 54% from 0.09 ± 0.02 to 0.04 ± 0.01. Even if the COF is halved, the wear rate remains unchanged and is of the same magnitude as the reference at 13.9 ± 2.8 (PA6.6) and $16.5 \pm 3.1 \times 10^{-6}\,\mathrm{mm}^3 \times (\mathrm{Nm})^{-1}$ (PA6.6 + PA/MC5). The specific wear rates are about a half as high as the wear rates of the PA6 samples.

Figure 17 shows 3D images of the wear track of the PA6.6 samples. The wear track of the microcapsule-filled sample is more pronounced compared with the unfilled sample. The wear depth is highest at the ends of the wear track. In comparison to the rotational analysis, the tested distance in oscillation is much lower at 20 m.

In order to estimate the effectiveness of microcapsule composites, it is necessary to conduct in-depth tribological tests. Despite tests over longer distance durations to obtain a more accurate evaluation of wear and friction; further counter-bodies are of great interest. Additional

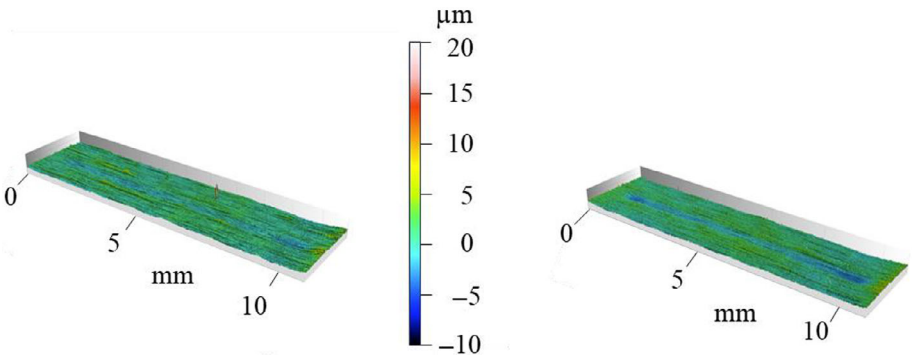

FIGURE 17 Microscopic 3D images of PA6.6 and microcapsules-filled PA6.6 (+PA/MC5) after tribological oscillation measurement tested against steel 100Cr6 ball. [Color figure can be viewed at wileyonlinelibrary.com]

investigations with other counter-body materials (ceramics and plastics), surface contact geometries, and roughness are of great interest in order to be able to evaluate the tribological potential better. External factors such as water droplets can result in the removal of the lubrication. The extent to which oil can be replenished by capillary effects can be analyzed based on the tests shown by Tran et al.[44]

4 | CONCLUSIONS

In this study, we demonstrate that the fabrication of self-lubricating PA6 and PA6.6 by extrusion and injection-molding is feasible and presents an exciting possibility for the reduction of friction and wear and related energetic losses in PA-based plastic parts and the extension of their service life. The production was demonstrated on kg-scale using a corotating twin-screw extruder system and an injection molding unit. The production of 100 tensile rods could be performed with unchanged process parameters. This represents a significant achievement in the transfer of scientific results into industrial applications and serves to demonstrate the high technology readiness level.

In order to achieve this result, highly thermally and mechanically stable lubricant-filled microcapsules with a cross-linked PA shell and a diameter of D_{90} 50 µm were synthesized by interfacial polymerization and isolated as the dry powder via spray-drying. The resulting microcapsules show high thermal stability (5 wt% weight loss at 350°C in TGA), which makes them suitable for the processing in PA melts (265°C). The tribological characterization of parts filled with microcapsules showed a significant reduction in both friction and wear values for PA6 samples, up to 80% and 56% respectively. The tribological performance of PA6.6 samples shows an opposite result, while the friction values are reduced in rotation and oscillation mode, the wear rate is reduced only in rotation. By using microcapsules in PA6.6, a reduction in COF (77%) and wear (75%) can be achieved in rotation. However, the use of microcapsule-filled compounds was found to result in a reduction in Young's modulus and tensile strength, which may limit their suitability for use in mechanically stressed parts.

AUTHOR CONTRIBUTIONS

Moritz Grünewald: Conceptualization (lead); funding acquisition (equal); investigation (equal); writing – original draft (lead); writing – review and editing (supporting). **David Herbig:** Investigation (equal); writing – original draft (supporting). **Michael Heilig:** Conceptualization (supporting); writing – original draft (supporting). **Johannes Rudloff:** Conceptualization (equal); project administration (lead); writing – review and editing (lead). **Martin Bastian:** Funding acquisition (lead); supervision (lead). **Gunnar Engelmann:** Funding acquisition (equal); supervision (equal); writing – review and editing (equal). **Max Hirsekorn:** Investigation (equal). **Alexandra Latnikova:** Conceptualization (lead); funding acquisition (equal); investigation (lead); supervision (equal); writing – original draft (equal); writing – review and editing (equal).

ACKNOWLEDGMENTS

This research is financially funded by the German Federal Ministry for Economic Affairs and Climate Action (BMWK) via the German Federation of Industrial Research Associations (AiF) as part of the program for the promotion of joint industrial research (IGF) (project-ID: 210707 BG). Open Access funding enabled and organized by Projekt DEAL.

CONFLICT OF INTEREST STATEMENT

The authors report there are no competing interests to declare.

DATA AVAILABILITY STATEMENT

The data that support the findings of this study are available from the corresponding author upon reasonable request.

ORCID

Moritz Grünewald https://orcid.org/0000-0003-3082-4919

Johannes Rudloff https://orcid.org/0000-0002-7436-6326

REFERENCES

[1] S. Kamerling, A. K. Schlarb, *Tribol. Int.* **2020**, *147*, 106271.
[2] Z. Raheem, A. A. Kareem, *Eng. Trans.* **2017**, *65*, 307.
[3] Y. Q. Tian, J. L. Huo, *AMM* **2012**, *182*, 135.
[4] Z. Yang, Z. Guo, C. Yuan, *Wear* **2019**, *432*, 102919.
[5] G. Lu, X. Yang, X. Qi, X. Yan, Y. Dong, W. Yao, L. Liang, *Tribol. Int.* **2022**, *173*, 107624.
[6] C. Georgescu, L. Deleanu, L. Chiper Titire, A. C. Ceoromila, *Materials*, **2021**, *14*, 997.
[7] T. Huang, R. Lu, H. Wang, Y. Ma, J. Tian, T. Li, *J. Macromol. Sci. B* **2011**, *50*, 1235.
[8] H. Zhang, Y. Wu, M. Liang, H. Wu, H. Zou, Y. Chen, S. Zhou, *J. Thermoplast. Compos. Mater.* **2020**, *35*, 1319.
[9] T. W. Scharf, S. V. Prasad, *J. Mater. Sci.* **2013**, *48*, 511.
[10] Z. Li, X. Qi, C. Liu, B. Fan, X. Yang, *Wear* **2023**, *532*, 205104.
[11] A. Saurabh, A. Manoj, T. Boni, T. R. Pradhan, U. Basavaraj, P. Saravanan, A. Kumar, R. Das, P. C. Verma, *Met. Mater. Int.* **2024**, *30*, 697.
[12] L. Lin, A. K. Schlarb, *Polym. Adv. Technol.* **2021**, *32*, 3150.
[13] N. K. Myshkin, M. I. Petrokovets, A. V. Kovalev, *Tribol. Int.* **2005**, *38*, 910.
[14] X. Yan, X. Yang, X. Qi, G. Lu, Y. Dong, C. Liu, B. Fan, *Tribol. Int.* **2022**, *166*, 107336.
[15] Q. B. Guo, K. T. Lau, B. F. Zheng, M. Z. Rong, M. Q. Zhang, *Macromol. Mater. Eng.* **2009**, *294*, 20.
[16] H. Li, S. Li, Z. Li, Y. Zhu, H. Wang, *Langmuir: ACS J. Surf. Colloids* **2017**, *33*, 14149.
[17] Y.-J. Mao, P.-P. Gao, Z.-B. Sun, J.-H. Tang, K. Dai, H. Lin, G.-J. Zhong, Z.-M. Li, *Ind. Eng. Chem. Res.* **2021**, *60*, 16023.
[18] B. Mu, Z. Jiang, B. Yang, J. Cui, X. Wang, J. Guo, X. Bao, L. Chen, *Polym. Eng. Sci.* **2018**, *59*, 490.
[19] M. Yang, X. Zhu, G. Ren, X. Men, F. Guo, P. Li, Z. Zhang, *Tribol. Lett.* **2015**, *58*, 9.
[20] H. Li, Y. Ma, Z. Li, J. Ji, Y. Zhu, H. Wang, *RSC Adv.* **2017**, *7*, 50328.
[21] M. Grünewald, A. Latnikova, K. Hohmann, A. Sänger, J. Rudloff, M. Bosse, T. Hochrein, M. Bastian, *innoTRAC* **2022**, *2*, 25.
[22] N. Espallargas, L. Vitoux, S. Armada, *Surf. Coat. Technol.* **2013**, *235*, 342.
[23] S. Armada, R. Schmid, S. Equey, I. Fagoaga, N. Espallargas, *J Therm. Spray Tech.* **2013**, *22*, 10.
[24] X. Li, H. Li, Z. Li, N. Shi, H. Luo, S. Li, C. Yu, *Polymer* **2023**, *281*, 126134.
[25] Z. Li, A. Luo, R. Zhou, X. Li, H. Li, *Polymer* **2024**, *290*, 126537.
[26] S. Apichartpattanasiri, J. N. Hay, S. N. Kukureka, *Wear* **2001**, *251*, 1557.
[27] H. Gong, C. Yu, L. Zhang, G. Xie, D. Guo, J. Luo, *Compos. B Eng.* **2020**, *202*, 108450.
[28] D. Poncelet, R. Leung, L. Centomo, R. J. Neufeld, *J. Chem. Technol. Biotechnol.* **1993**, *57*, 253.
[29] J. J. Ayerdi, A. Aginagalde, I. Llavori, J. Bonse, D. Spaltmann, A. Zabala, *Wear* **2021**, *470-471*, 203620.
[30] J. Sun, Y. Wang, N. Li, L. Tian, *Tribol. Int.* **2019**, *136*, 332.
[31] N. W. Khun, H. Zhang, C. Y. Yue, J. L. Yang, *J. Appl. Mech.* **2014**, *81*, 071004.
[32] S. Aziz, J. Gill, P. Dutilleul, R. Neufeld, S. Kermasha, *J. Microencapsulation* **2014**, *31*, 774.
[33] A. D. Mytara, K. Chronaki, V. Nikitakos, C. D. Papaspyrides, K. Beltsios, S. Vouyiouka, *Materials* **2021**, *14*, 5895.
[34] W. Chen, X. Liu, D. W. Lee, *J. Mater. Sci.* **2012**, *47*, 2040.
[35] P. Hu, E. M. Hadji, T. Shi, M. Tai, J. Wang, *ChemistrySelect* **2019**, *4*, 6917.
[36] B. C. Smith, *Spectroscopy* **2022**, *37*, 15.
[37] Mocom Compounds GmbH & Co. *KG. ALCOM PA6 900/1 PTFE10 IM Technisches Merkblatt*, Mocom GmbH, Hamburg **2024**. Available online: https://www.mocom.eu/en/products/download/doc/de/SI/albis/ALCOMPA69001PTFE10IM.pdf (accessed on 17 May 2024).
[38] B. M. Rudresh, B. N. Ravikumar, *Trans. Indian Inst. Met.* **2017**, *70*, 1285.
[39] N. Win Khun, H. Zhang, X. Tang, C. Yoon Yue, J. Yang, *J. Appl. Mech.* **2014**, *81*, 121004.
[40] S. V. Panin, V. O. Alexenko, D. G. Buslovich, *Polymer* **2022**, *14*, 975.
[41] L. Du-Xin, L. Wen-Juan, X. Ying, L. Xiang-Xiang, *J. Appl. Polym. Sci.* **2012**, *124*, 4239.
[42] S. Sathees Kumar, G. Kanagaraj, *Arab J. Sci. Eng.* **2016**, *41*, 4347.
[43] H.-G. Wang, L.-Q. Jian, B.-L. Pan, J.-Y. Zhang, S.-R. Yang, *Polym. Eng. Sci.* **2007**, *47*, 738.
[44] H.-H. Tran, Y. Kim, C. Ternon, M. Langlet, D. Riassetto, D. Lee, *Adv. Mater. Int.* **2021**, *8*, 2002058.

How to cite this article: M. Grünewald, D. Herbig, M. Heilig, J. Rudloff, M. Bastian, G. Engelmann, M. Hirsekorn, A. Latnikova, *J. Appl. Polym. Sci.* **2024**, *141*(35), e55894. https://doi.org/10.1002/app.55894